Electronic Supplementary Material (ESI) for Physical Chemistry Chemical Physics.

Monolayer Molybdenum Diborides containing Flat and Buckled Boride Layers as Anode Materials for Lithium-Ion Batteries

Gayatree Barik[1,2] and Sourav Pal* [1,2]

[1]*Department of Chemical Sciences, Indian Institute of Science Education and Research Kolkata, Mohanpur-741 246, India*

[2]*Department of Chemistry, Ashoka University, Sonepat, Haryana-131 029, India*

Email: sourav.pal@ashoka.edu.in

Fig. S1: (i) Top and side view of various Li adsorption sites on the surface of $P6/mmm$ MoB_2. (a) Hexagonal hollow site of Boron, (b) Boron Top, (c) Hollow position of Mo, (d) and Top position of Mo. The blue, green, and red balls represent the Mo, B, and Li atoms, respectively.

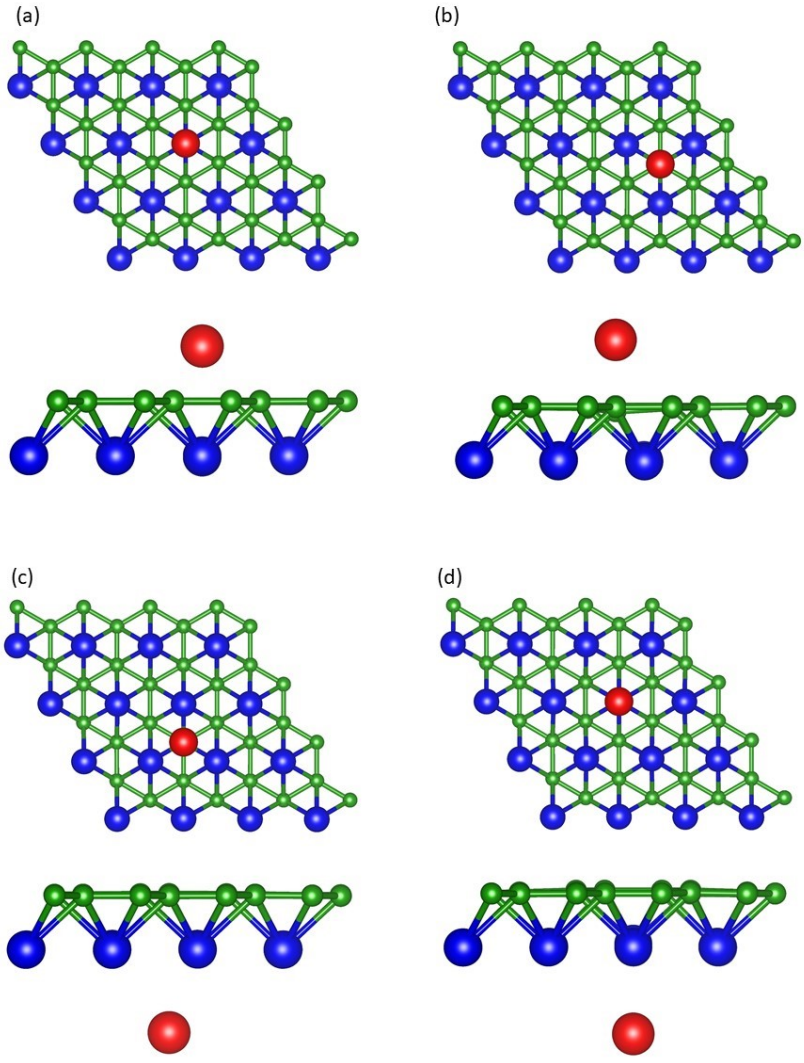

Fig. S1(ii): Top and side view of various Li adsorption sites on the surface of $R\bar{3}m$ MoB_2. (a) Hexagonal hollow site of Boron, (b) Boron Top, (e) Furo position of B, (d) Hollow position of Mo, (e) Li at the center of three B and top of Mo (f) Li at the center of three Mo and top of B. The blue, green, and red balls represent the Mo, B, and Li atoms, respectively.

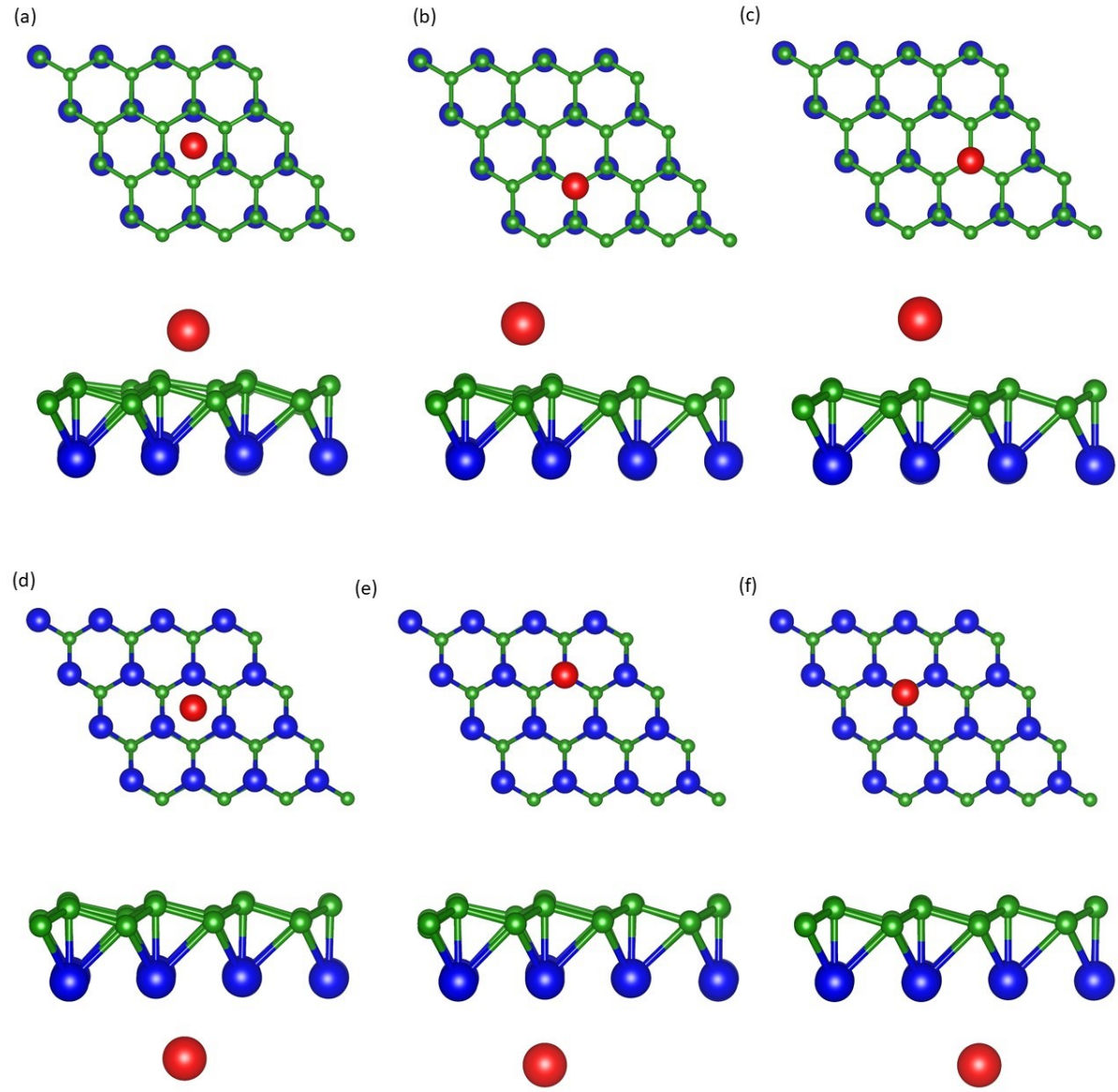

Fig. S2: (i) The strain-energy curves for the calculation of in-plane stiffness constants for $P6/mmm$ Li_2MoB_2. The total energy of MoB_2 is plotted as a function of different amounts of strain along (a) the x-axis, (b) the y-axis, and (c) equi-biaxial strain along the x and y-axis, necessary for the calculation of in-plane stiffness constants.

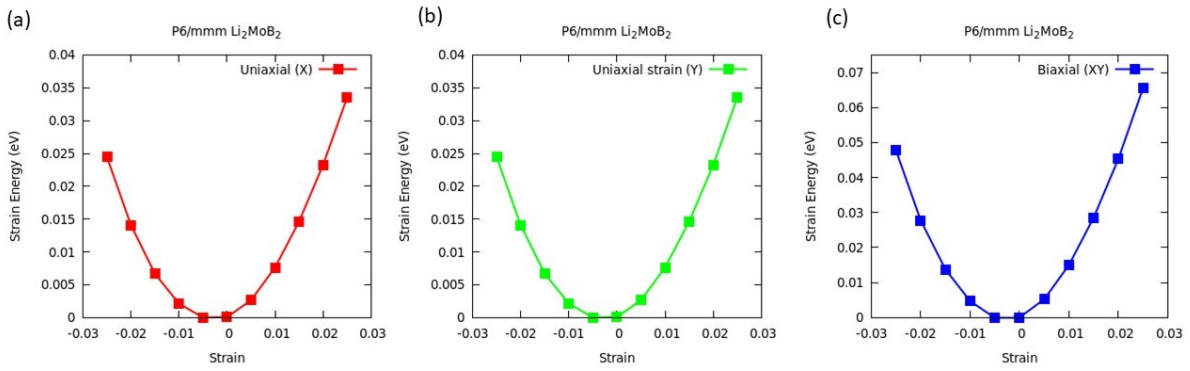

Fig. S2: (ii) The strain-energy curves for the calculation of in-plane stiffness constants for $R\bar{3}m$ Li_2MoB_2. The total energy of MoB_2 is plotted as a function of different amounts of strain along (a) the x-axis, (b) the y-axis, and (c) equi-biaxial strain along the x and y-axis, necessary for the calculation of in-plane stiffness constants.

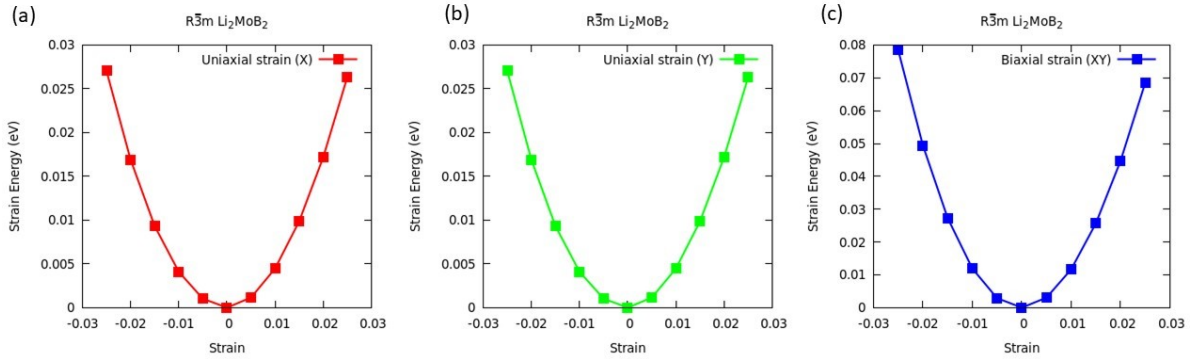

Fig. S2: (iii) The strain-energy curves for the calculation of in-plane stiffness constants for $P6/mmm$ Li_4MoB_2. The total energy of MoB_2 is plotted as a function of different amounts of strain along (a) the x-axis, (b) the y-axis, and (c) qui-biaxial strain along the x and y-axis, necessary for the calculation of in-plane stiffness constants.

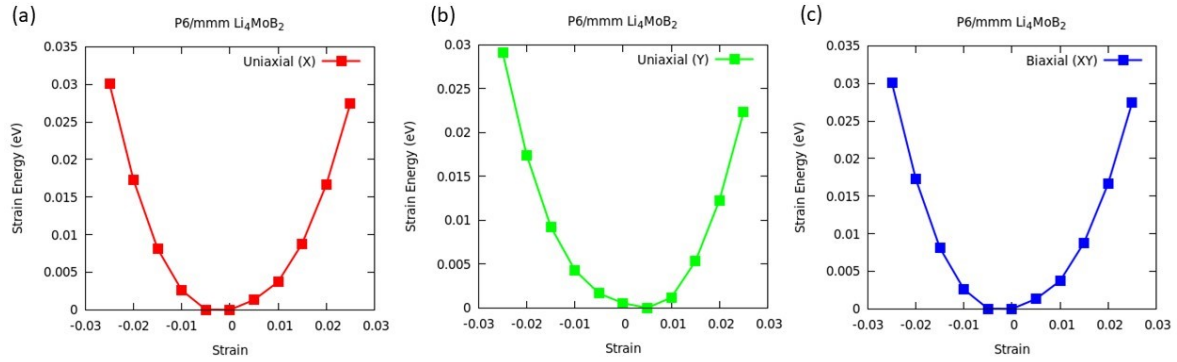

Fig. S2: (iv) The strain-energy curves for the calculation of in-plane stiffness constants for $R\bar{3}m$ Li_4MoB_2. The total energy of MoB_2 is plotted as a function of different amounts of strain along (a) the x-axis, (b) the y-axis, and (c) Equi-biaxial strain along the x and y-axis, necessary for the calculation of in-plane stiffness constants.

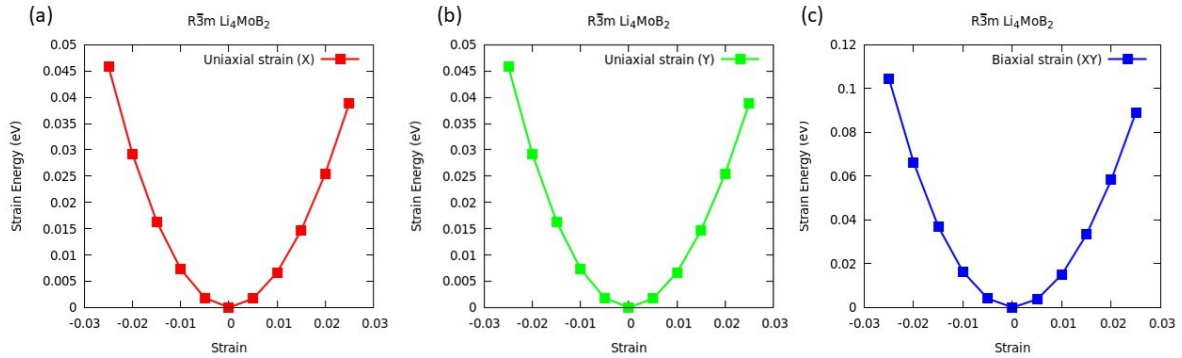

Fig. S3 (i): Top and side view of optimized geometries of Li adsorption with different Li concentrations adsorbed on both sides of $P6/mmm$ MoB_2. (a) $Li_{0.5}MoB_2$ (b) $LiMoB_2$ (c) Li_2MoB_2 and (d) Li_4MoB_2.

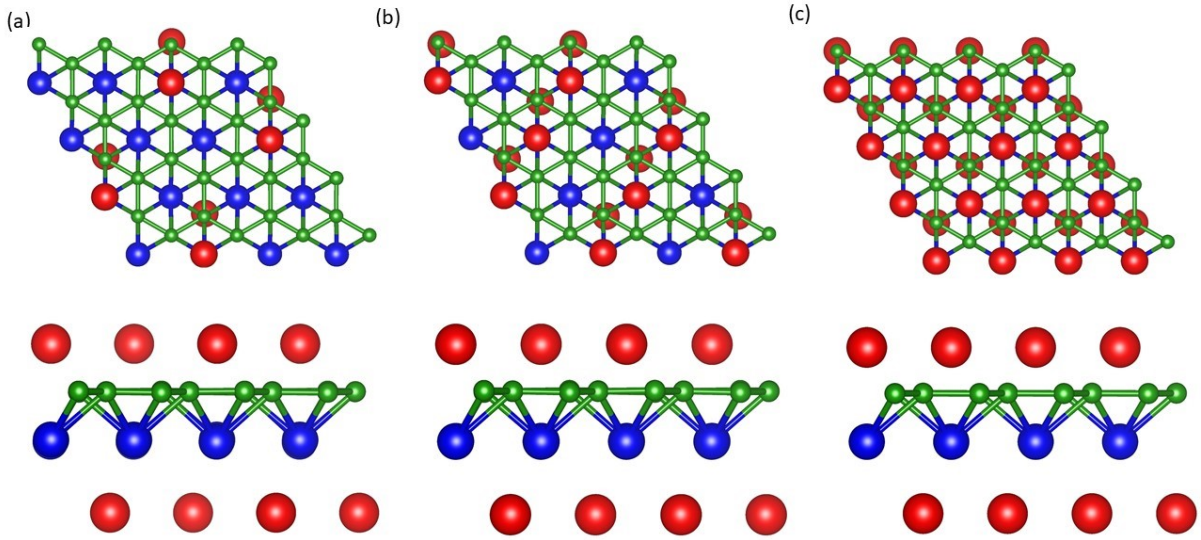

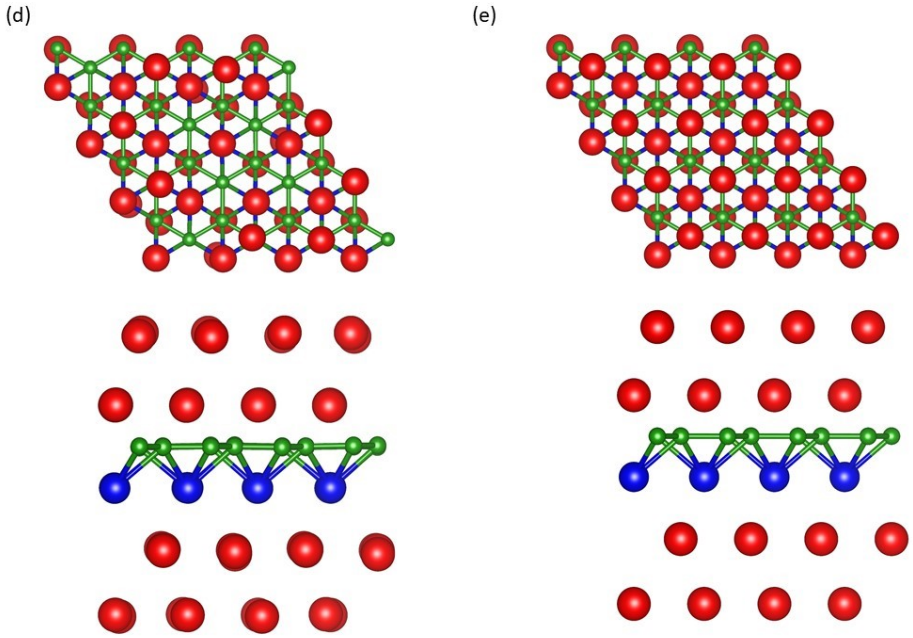

Fig. S3 (ii): Top and side view of optimized geometries of Li adsorption with different Li concentrations adsorbed on both sides of $R\bar{3}m$ MoB_2. (a) $Li_{0.5}MoB_2$ (b) $LiMoB_2$ (c) Li_2MoB_2 (d) Li_3MoB_2 and (e) Li_4MoB_2.

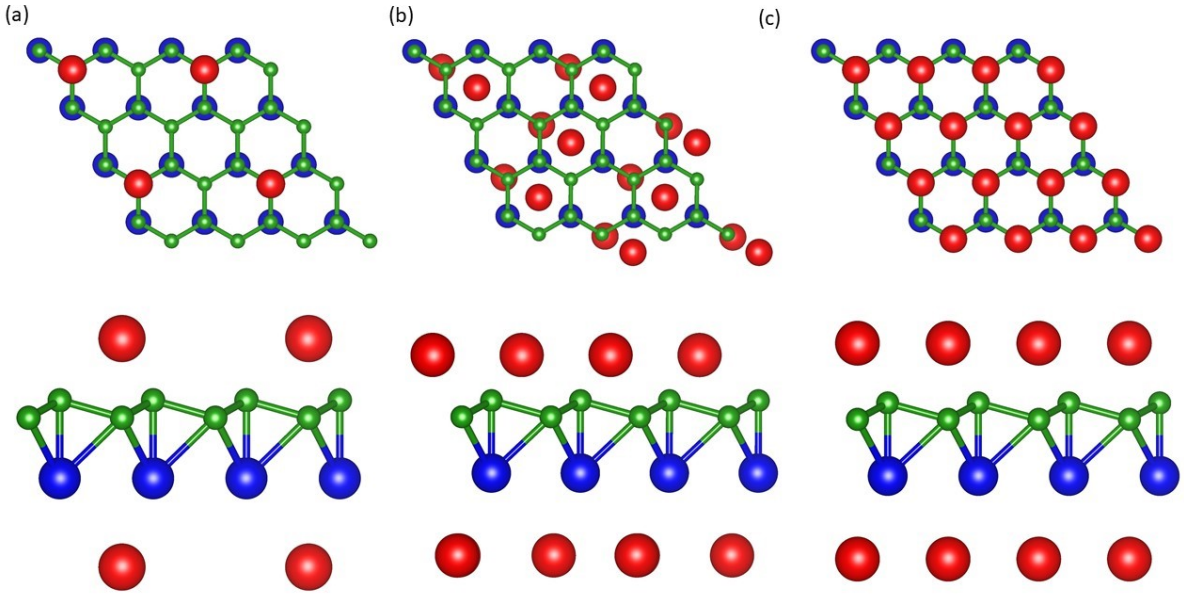

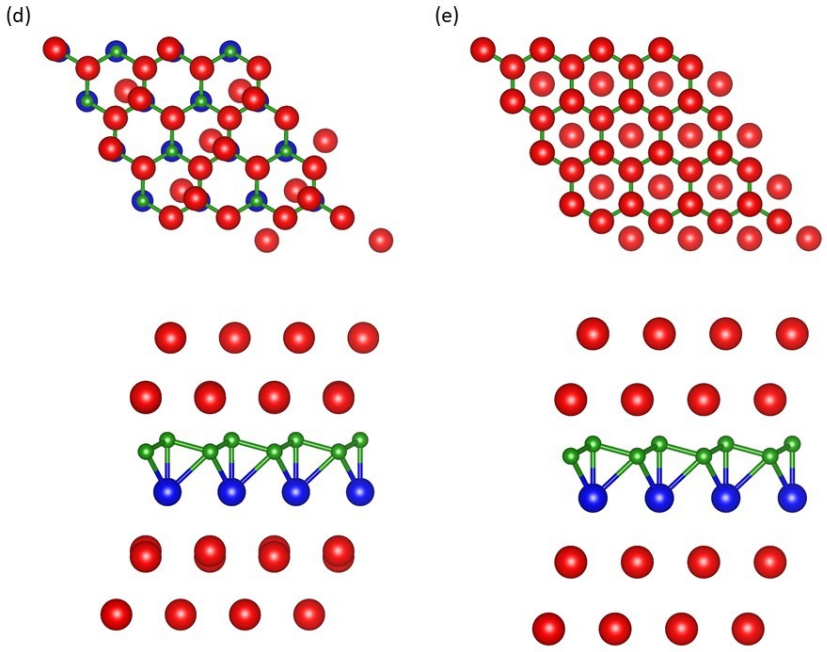

Fig. S4 (i): The fluctuation of total potential energy and snapshots taken at the end of MD simulations at 300 K (a) $P6/mmm$ and (b) $R\bar{3}m$ Li_2MoB_2 and at 500 K (c) $P6/mmm$ and (d) $R\bar{3}m$ Li_2MoB_2.

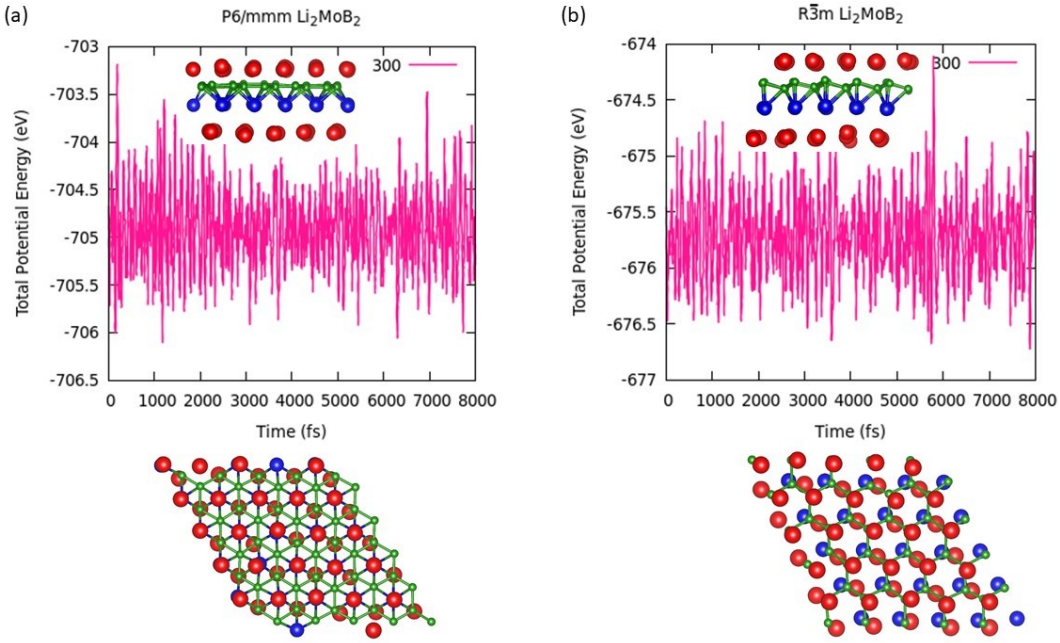

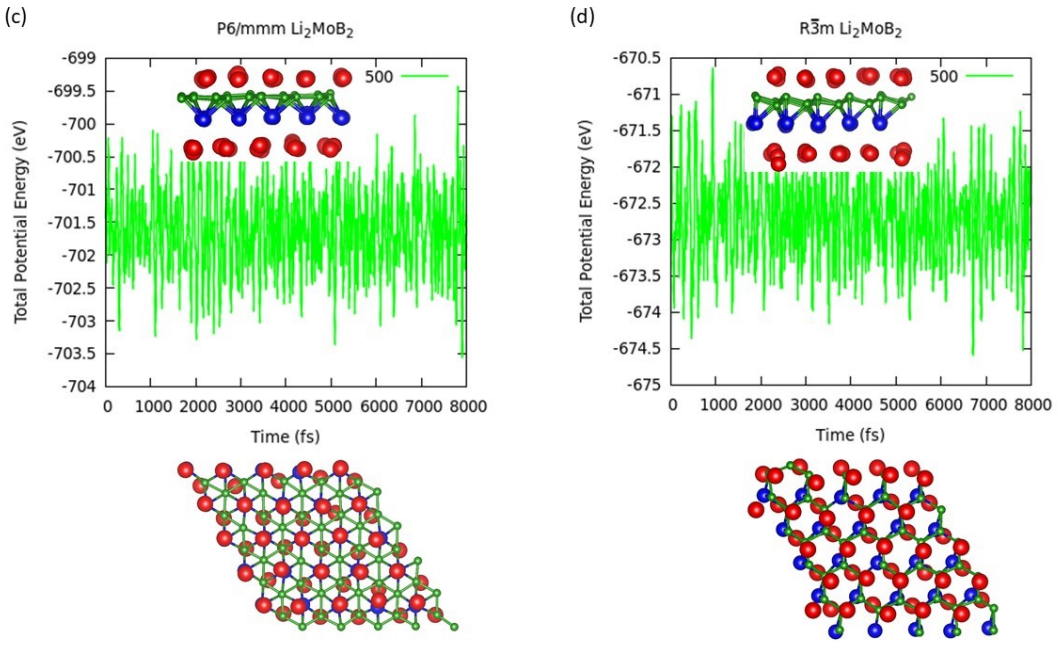

Fig. S4 (ii): The fluctuation of total potential energy and snapshots taken at the end of MD simulations at 300 K (a) $P6/mmm$ and (b) $R\bar{3}m$ Li_4MoB_2 and 500 K (c) $P6/mmm$ and (d) $R\bar{3}m$ Li_4MoB_2.

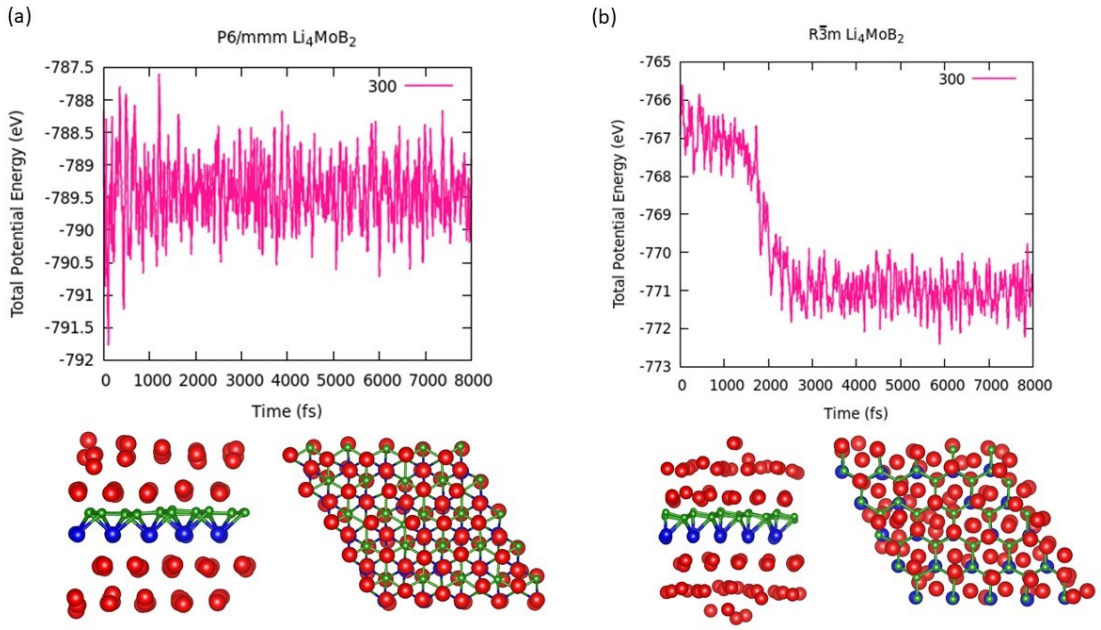

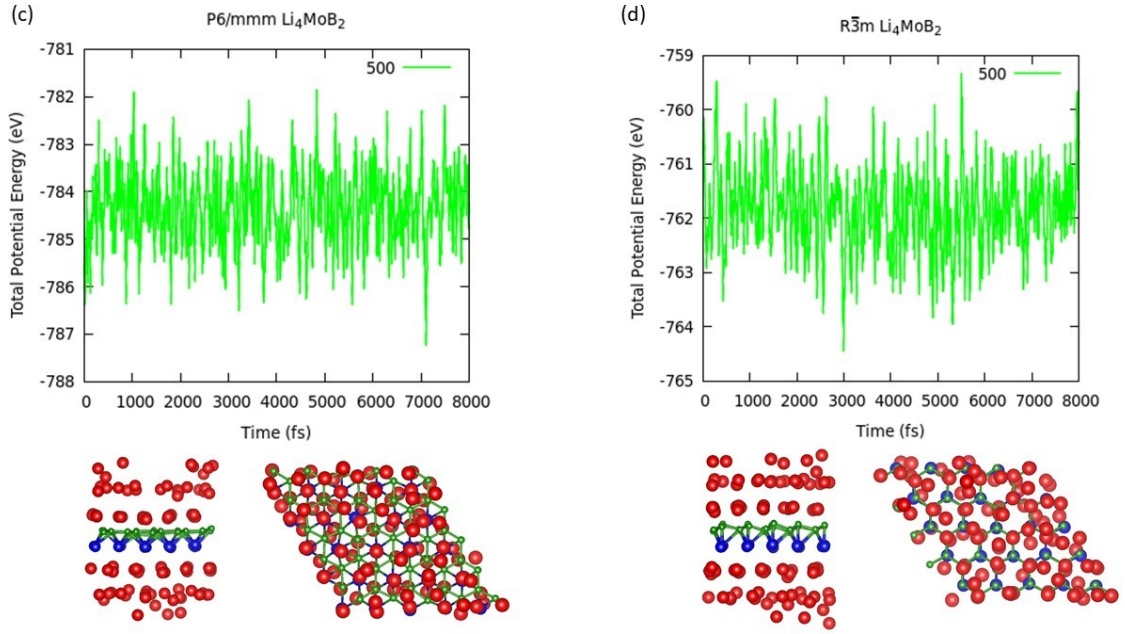

Fig. S5 (i): Energy barriers and diffusional pathways for the diffusion of Li over monolayer $P6/mmm$ MoB_2 along the non-linear paths at the various surfaces.

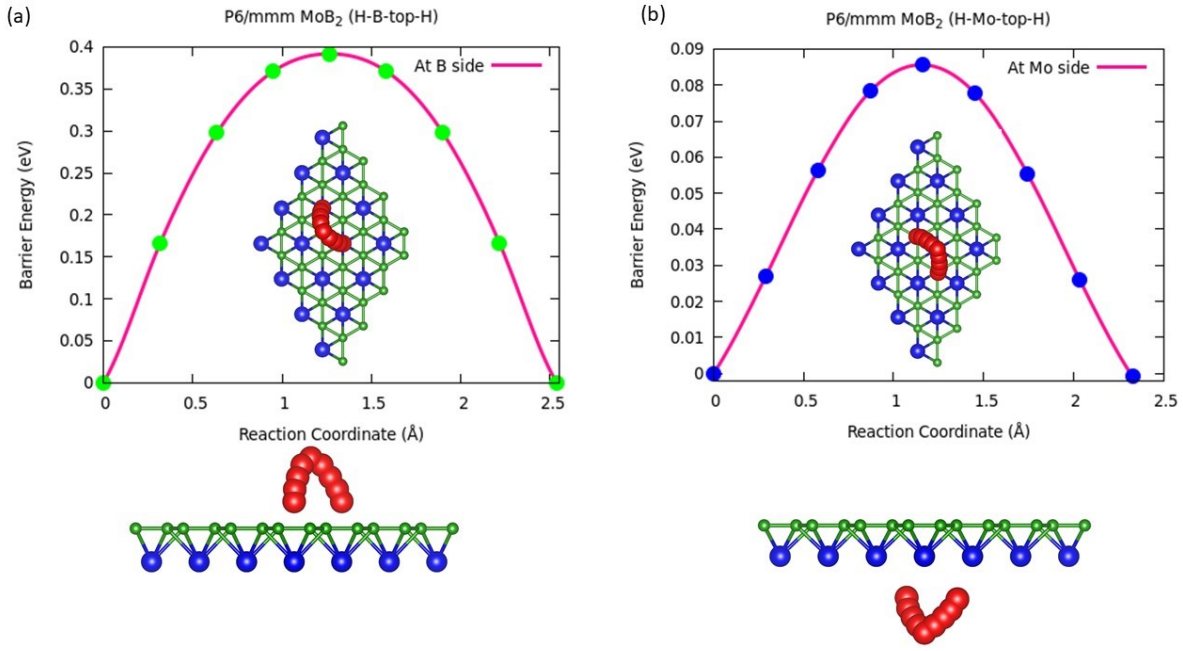

Fig. S5 (ii): Energy barriers and diffusional pathways for the diffusion of Li over monolayer $R\bar{3}m$ MoB_2 along the non-linear paths at the various surfaces.

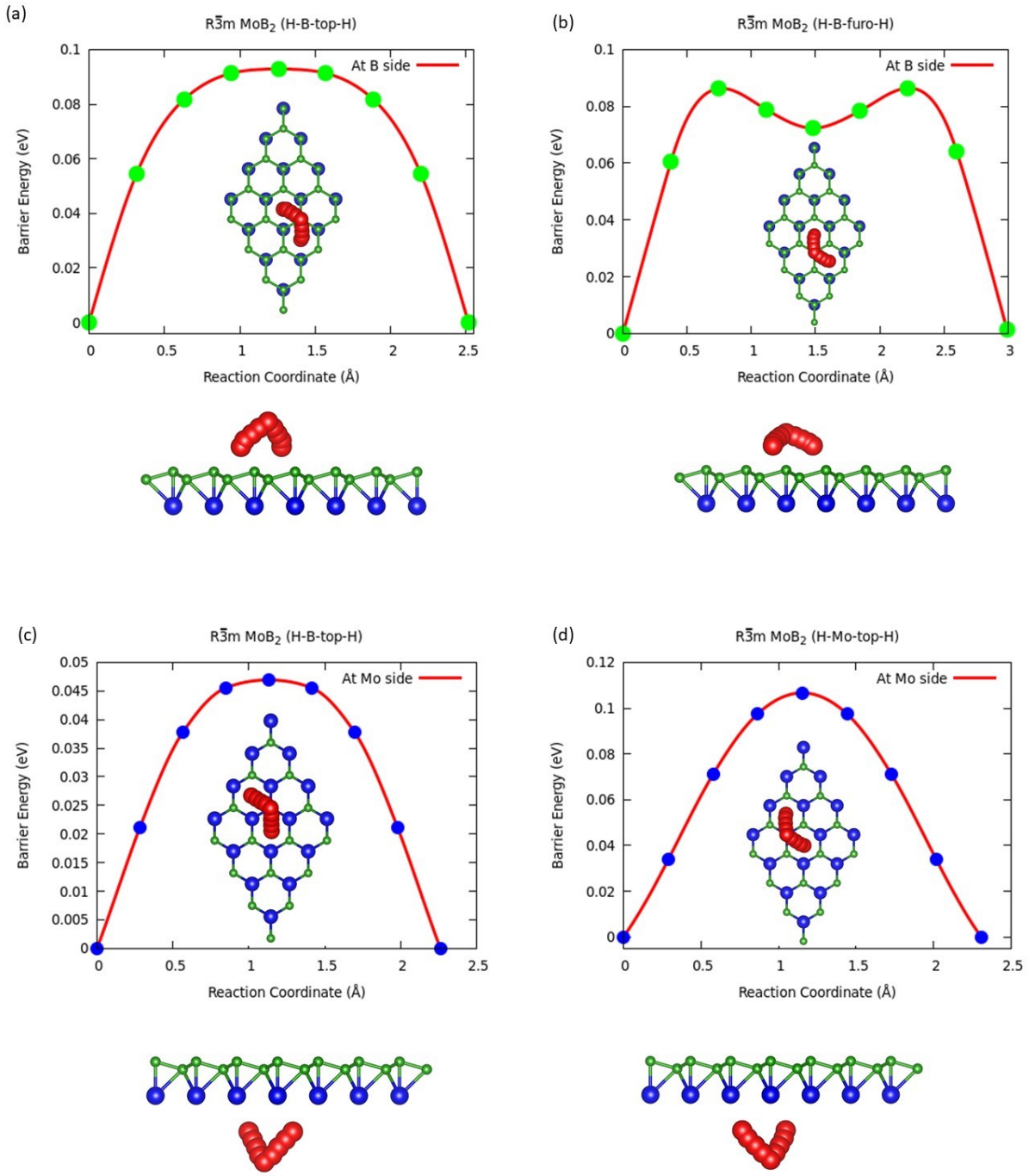

Table S1 (i): The specific lattice information for *P6/mmm* MoB_2 and $R\bar{3}m$ MoB_2.

	P6/mmm MoB_2	$R\bar{3}m$ MoB_2
Space group	*P6/mmm*	$R\bar{3}m$
Space group Number	191	166
Lattice parameters (Å)	a= 2.91 c= 3.37	a=2.86 c=20.93

Wyckoff positions	Mo: (1a) 0.00 0.00 0.00 B : (2d) 0.333 0.666 0.50	Mo: (6c) 0, 0, 0.5758 B: (6c) 0, 0, 0.6817 B: (6c) 0, 0, 0.1677

Table S1 (ii): The atomic coordinates for *P6/mmm* MoB_2 and $R\bar{3}m$ MoB_2.

P6/mmm MoB_2	0.583313584 0.916652739 0.250016809	0.916652739 0.583313584 0.250016809	0.551014364 0.551014364 0.448985666
$R\bar{3}m$ MoB_2	0.333333790 0.666666269 0.333333731	0.666666210 0.333333731 0.666666269	0.560779035 0.533561826 0.439220965

Table S2 (i): The impact cut-off energy on the adsorption energy and band gap. The hexagonal hollow position is chosen for the lithiation of both monolayers. The adsorption of Li takes place at the hexagonal position of the B-side of both monolayers. The negative values of band gaps for the *P6/mmm* MoB_2 show the overlapping of VMB and CBM.

Ecut in eV	*P6/mmm* MoB_2		$R\bar{3}m$ MoB_2	
	AE in eV	Bandgap in eV	AE in eV	Bandgap in eV
400	-4.297	-0.603	-3.783	0.224
420	-4.297	-0.603	-3.779	0.224
440	-4.298	-0.603	-3.779	0.224
460	-4.299	-0.603	-3.779	0.224
480	-4.302	-0.602	-3.774	0.224
500	-4.302	-0.602	-3.776	0.224

Table S2 (ii): The impact of vacuum thickness with adsorption energy. The hexagonal hollow position is chosen for the lithiation of both monolayers.

Vacuum (Å)	Adsorption Energy (eV)	
	P6/mmm MoB_2	$R\bar{3}m$ MoB_2
10	-4.24	-3.74
15	-4.29	-3.76
20	-4.32	-3.76
25	-4.33	-3.77

30	-4.34	-3.77

Table S3 (i): The calculated adsorption energy with and without dispersion corrections, for *P6/mmm* MoB_2 and $R\bar{3}m$ MoB_2 at various positions.

Adsorption Location	Adsorption Energy (eV)			
	P6/mmm MoB_2		$R\bar{3}m$ MoB_2	
	DFT without dispersion correction	DFT+D3	DFT without dispersion correction	DFT+D3
B(Hollow)	-3.99	-4.22	-3.57	-3.88
B(Top)	-3.46	-3.70	-3.23	-3.53
B (Furo)	---	---	-2.82	-3.10
Mo (Hollow)	-2.61	-2.78	-2.57	-2.75
Mo (Top)	-2.50	-2.70	-2.44	-2.63
Mo (B top)	---	---	-2.48	-2.67

Table S3 (ii): The calculated adsorption energy with and without Hubbard parameter, for *P6/mmm* MoB_2 and $R\bar{3}m$ MoB_2 at various positions.

Adsorption Location	Adsorption Energy (eV)			
	P6/mmm MoB_2		$R\bar{3}m$ MoB_2	
	DFT	DFT+*U*	DFT	DFT+*U*
B(Hollow)	-4.21	-4.22	-3.78	-3.88
B(Top)	-3.69	-3.70	-3.44	-3.53
B (Furo)	---	---	-3.00	-3.10
Mo (Hollow)	-2.78	-2.78	-2.73	-2.75
Mo (Top)	-2.68	-2.70	-2.62	-2.63
Mo (B top)	---	---	-2.65	-2.67

Table S4(i): The calculated Li migration barrier and Li-Vacancy barrier for the diffusion of Li at the various surfaces of flat and buckled MoB_2.

MoB_2	Li-ion migration barrier energy in	Li-vacancy migration barrier

	eV		energy in eV	
	At B side	At Mo side	At B side	At Mo side
$P6/mmm$ MoB_2	0.52	0.02	0.90	0.20
$R\bar{3}m$ MoB_2	0.36	0.08	0.39	0.29

Table S4(ii): The calculated Li migration barrier and Li-Vacancy barrier for the diffusion of Li along the non-linear paths at the various surfaces of flat and buckled MoB_2.

MoB_2		Li-ion migration barrier energy in eV along the non-linear path	
		At B side	At Mo side
$P6/mmm$ MoB_2		0.391	0.085
$R\bar{3}m$ MoB_2	Path I	0.092	0.047
	Path II	0.086	0.105